DESIGN AND TEST OF PATH TRACKING CONTROL SYSTEM FOR SOYBEAN WEEDING ROBOT
/
大豆除草机器人路径跟踪控制系统设计与试验

Nai-chen ZHAO[1)], Gang CHE*[1,2)], Lin WAN[1,2)], Shuai ZANG[1)], Chun-sheng WU[3)] Zong-jun GUO[1)]
[1)] College of Engineering, Heilongjiang Bayi Agricultural University, Daqing 163319, China
[2)] Key Laboratory of Intelligent Agricultural Machinery Equipment in Heilongjiang Province, Daqing 163319, China
[3)] Jiamusi Branch of Heilongjiang Academy of Agricultural Machinery Sciences, Jiamusi 154004,China
Tel:+86-459-13836961617;E-mail: chegang180@126.com
Corresponding author: Gang CHE
DOI: https://doi.org/10.35633/inmateh-77-122

Keywords: *LADRC, Pure Pursuit algorithm, INGO optimization, speed stability control, lateral error reduction*

ABSTRACT
To mitigate tracking degradation caused by unstable speeds in weeding robots, this study integrates Linear Active Disturbance Rejection Control (LADRC) with the Pure Pursuit (PP) algorithm. An Improved Northern Goshawk Optimization (INGO) algorithm is employed to optimize the LADRC parameters, enabling more precise speed regulation. Field experiments conducted at speeds of 0.5, 0.8, and 1.0 m/s compared the proposed approach with a conventional PID-PP controller. The results demonstrate that the proposed method reduced the maximum lateral tracking error by 9.67%, 19.0%, and 20.5%, respectively, while consistently improving both MAE and RMSE. These findings confirm that the proposed control strategy effectively enhances path tracking stability and precision, thereby improving the autonomous navigation performance of weeding robots.

摘要
为解决除草机器人因速度不稳定导致的路径跟踪性能下降问题，本文将线性自抗扰控制（LADRC）与纯追踪（PP）相结合。利用改进的北方苍鹰优化算法（INGO）优化 LADRC 参数以实现精确的速度控制。在 0.5、0.8 和 1.0 m/s 速度下的田间试验表明，与 PID-PP 控制器相比，该方法将最大横向误差分别降低了 9.67%、19.0% 和 20.5%，且 MAE 和 RMSE 均持续改善。结果证实该算法有效提升了自动除草作业的路径跟踪稳定性与精度。

INTRODUCTION

Soybean, as a crucial food, oilseed, and feed crop in China, holds an irreplaceable strategic position in ensuring national food security, maintaining edible oil supply, and supporting sustainable livestock development *(Liu et al., 2025)*. Heilongjiang Province accounts for over 40% of China's total soybean yield and cultivated area, making it the major soybean producing region nationwide. With increasing attention to green and organic certified foods, the cultivated area of such soybeans has continuously expanded. Compared to conventional soybean cultivation, green and organic production requires multiple weeding operations. However, traditional tractor-drawn weeding machinery presents problems such as soil compaction and high labor intensity. Therefore, developing intelligent weeding robots is significant for improving mechanical weeding quality and reducing labor costs.

The autonomous operation system of agricultural machinery comprises automatic navigation control and automatic operation control *(Liu et al., 2018)*. As a critical component, navigation tracking control has received widespread research attention. Classic control algorithms include Pure Pursuit *(Macenski et al., 2023; Ahn et al., 2021; Jain et al., 2024)*, Stanley *(AbdElmoniem et al., 2020; Wang et al., 2022)*, PID *(Deshmukh et al., 2025; Farag et al., 2020)*, LQR *(Ni et al., 2022)*, and Model Predictive Control *(Peicheng et al., 2022; Rokonuzzaman et al., 2023)*. The Pure Pursuit algorithm, with its simple structure and fast response speed, is widely used in agricultural machinery navigation systems with relatively low operating speeds.

Nai-chen Zhao, Ph.D. Stud. Eng.; Gang Che, Prof. Ph.D. Eng.; Lin Wan, Prof. Ph.D. Eng.; Shuai Zang, M.S. Stud. Eng.; Chun-sheng Wu, Engineer; Zong-jun Guo, M.S. Eng.

However, it has limitations including the inability to adjust look-ahead distance in real time and low tracking accuracy at high speeds.

Researchers have recently proposed improvements to the Pure Pursuit algorithm. *Xiao et al. (2023)* designed a segmented Pure Pursuit control algorithm adapting to different turning radii and lateral errors, improving path tracking accuracy by 30.9%, though the switching process reduced system response speed. *Shen et al. (2024)* corrected RTK coordinates and used an evaluation function quantifying errors to search for the optimal target point, obtaining the optimal look-ahead distance. *Li et al. (2013)* utilized fuzzy rules to adaptively determine look-ahead distance online. *Zhang et al. (2021)* designed a fuzzy adaptive Pure Pursuit control system for a tracked rapeseed direct seeder. *Pan et al. (2022)* introduced a front wheel compensation angle using a fuzzy-like method. *Zhang et al. (2016)* proposed a Pure Pursuit method based on a support vector regression inverse model, improving straight-line path tracking capability. *Zhang et al. (2020)* and *Fu et al. (2023)* determined look-ahead distance in real-time based on improved particle swarm optimization, improving driving accuracy. *Li et al. (2018)* incorporated real-time operating speed and target path curvature into the look-ahead distance relationship, dynamically adjusting it to improve algorithm accuracy. *Yang et al. (2022)* established an evaluation function for finding the optimal target point based on kinematic models and adaptively adjusted the look-ahead distance.

This study develops a compact weeding robot for ridge-planting soybean cultivation in Northeast China. To improve path tracking accuracy, a navigation control system based on the LADRC-PP algorithm is developed. Simulation experiments comparatively analyze the improved and original controllers. Field experiments verify the control system's stability, providing a foundation for subsequent robot development.

MATERIALS AND METHODS

Determination of Technical Specifications

Soybean cultivation in Northeast China commonly uses a high-platform ridge planting pattern. The ridges measure 1.1 m in width and 0.2–0.25 m in height. Depending on the characteristics of different soybean varieties, two or three rows are planted on each ridge, with an inter-row spacing of 0.420–0.450 m. Field weed control involves multiple operations, combining manual hoeing and mechanical cultivation. Mechanical weeding is conducted 3–4 times from pre-emergence to the first trifoliate leaf stage. During the growing season, manual weeding is performed three times, followed by one manual removal of large weeds in the late growth stage.

Structure and Working Principle

Based on these parameters, the weeding robot's chassis and weeding unit structures are designed. The main parameters of the chassis are shown in Table 1:

Table 1

Chassis main parameters

Parameter	Value
Overall dimensions (m × m × m)	2.2×1.3×1
Traveling mode	Wheeled
Drive wheel radius（m）	0.425
Wheel track（m）	1.1
Wheelbase（m）	1.1
Ground clearance（m）	0.425
Total mass（kg）	300.5
Drive motor power (kW)	3
Maximum speed（m/s）	1

Working Principle

The weeding robot drives the chassis through a DC brushless motor coupled with a reducer connected to the drive shaft. Steering is achieved by a stepper motor and reducer driving the steering mechanism. The weeding lifting module uses an electric push rod to adjust the lifting structure, and weeding operations can be performed by mounting different weeding units. The entire machine consists of a drive system, steering system, power module, visual recognition module, wireless remote control module, lifting module, and weeding module. The three-dimensional structure of the complete machine is shown in Fig. 1.

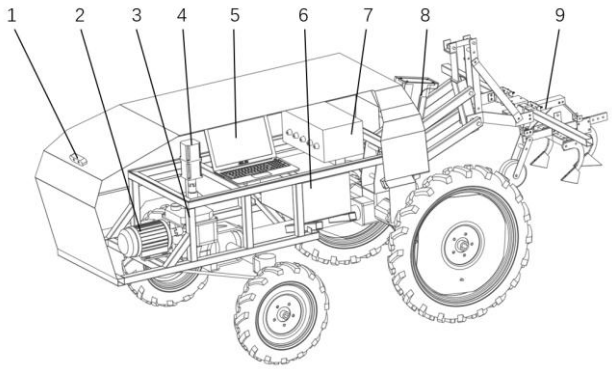

Fig. 1 - Schematic diagram of weeding robot structure
1- Camera; 2- DC brushless motor; 3- Reduction gearbox; 4- Steering motor; 5- Host computer; 6- Battery box; 7- Control box; 8- Lifting push rod; 9- Weeding unit

Structure Composition of Autonomous Operation System

The autonomous operation system of the weeding robot mainly consists of an information acquisition module, a control module, a motion module, and a weeding execution module. The working principle is shown in Fig. 2. The information acquisition module mainly consists of a camera and a front wheel angle sensor; the control module consists of a laptop computer, a wireless remote controller, and an STM32 microcontroller; the motion module and weeding execution module consist of DC brushless motors, stepper motors, motor drivers, and lifting electric push rods.

During weeding, a camera continuously captures seedling row images. A laptop computer uses deep learning algorithms to identify seedling rows and extract navigation lines, extracting lateral and heading deviations between the robot's path and the navigation line. This deviation data is sent to a microcontroller unit (MCU). The MCU then applies a path tracking control algorithm to generate real-time control signals, adjusting the front wheel steering angle and operational speed for accurate path tracking. The relationship between the motor rotational speed and the weeding robot's operational speed is as follows:

$$v = \frac{n*\pi*d}{60k} \quad (1)$$

where: n is the motor speed [r/min]; d is the drive wheel diameter[m]; k is the reducer reduction ratio; and v is the speed [m/s].

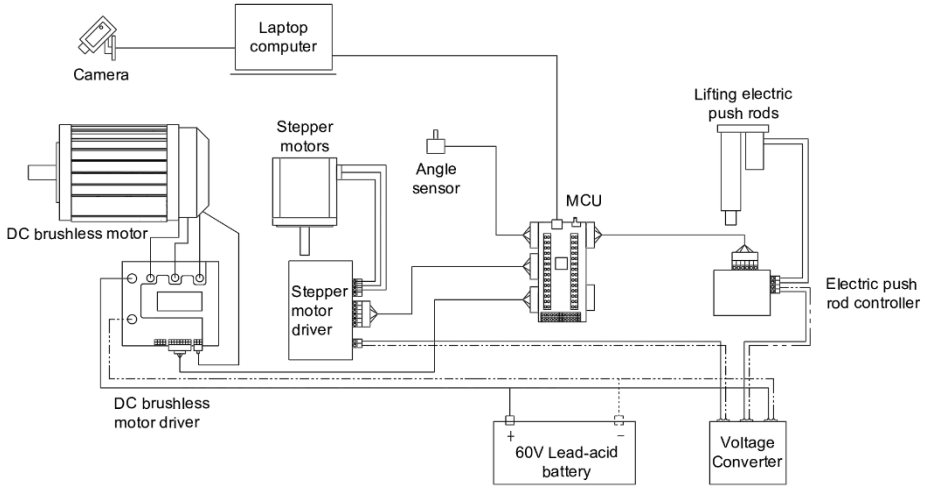

Fig. 2 - Schematic diagram of working principle of weeding robot

Navigation Controller Design

The weeding robot designed in this study employs an Ackermann steering model, where the left and right wheels exhibit identical motion characteristics. Considering the relatively flat terrain of Northeast China's soybean fields and the robot's low-speed, small-angle adjustments during operation, sideslip effects are neglected. The weeding robot is simplified into a two-wheel model, where the centers of the front and rear axles are hypothetically represented as single wheels to describe their respective motions *(Wang et al., 2019)*. The two-wheel model is illustrated in Fig. 3.

The control system of the two-wheel kinematic model alters the vehicle's position and heading by controlling the input velocity v_d and front wheel steering angle θ. Its kinematic model can be expressed as:

$$\begin{cases} \varphi = \frac{v_d}{R} = \frac{v_d \tan\delta}{L} \\ x_d = v_d \cos\theta \\ y_d = v_d \sin\theta \end{cases} \quad (2)$$

where:

φ is the Yaw angular velocity; x_d is the X-axis velocity component; and y_d is the Y-axis velocity component.

The Pure Pursuit algorithm is a geometry-based path tracking control method primarily applied in agricultural machinery operating at low speeds. It selects a target point on the desired path at a look-ahead distance from the vehicle's rear axle center. During operation, sensors continuously calculate the robot's lateral and heading deviations from the desired path, then compute the required front wheel steering angle for path tracking *(Zhang et al., 2020)*.

The Pure Pursuit model is illustrated in Fig. 4. In the figure, P represents the planar coordinate position of the weeding robot, Pd is the look-ahead point, Rd is the turning radius to reach the desired path, L_d is the look-ahead distance, α is the deviation angle between the vehicle body and the target path point, k is the path curvature to reach the desired path point, θ is the heading deviation between the weeding robot and the desired path, and d is the lateral deviation between the weeding robot and the desired path.

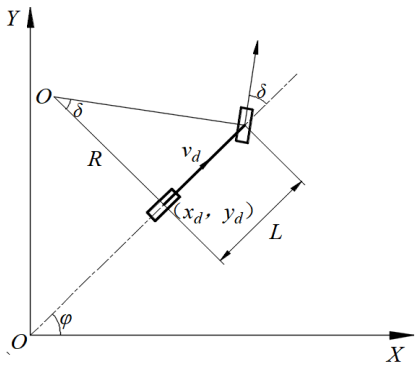

Fig. 3 - Two-wheeler model

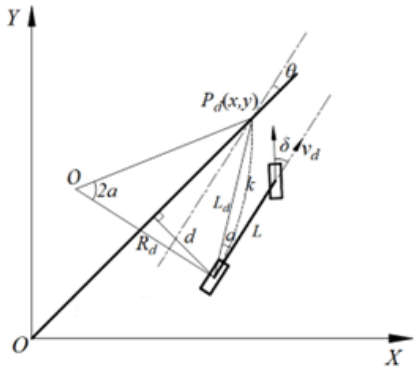

Fig. 4 - Pure tracking model

According to the geometric relationship in Figure 4, the curvature of the arc to the target point is determined by the look-ahead distance L_d and the lateral error d. By combining the Ackerman steering geometry, the final front wheel steering angle required for path tracking can be expressed as *(Zhang et al., 2020)*:

$$\delta = \frac{arctan(2L(d\cos\theta - \sqrt{L_d^2 - d^2\sin\theta}))}{L_d^2} \quad (3)$$

where: δ is the front wheel steering angle.

The equation above shows that the front wheel steering angle control variable depends on the look-ahead distance L_d, lateral error d, and heading error θ. During weeding, d and θ are calculated from the deviation between the seedling row navigation line (captured by the robot's camera) and its current position. Thus, L_d is the sole adjustable parameter in the Pure Pursuit model, and its proper selection enhances path tracking stability.

According to the geometric characteristics of the Pure Pursuit model, a small look-ahead distance L_d increases lateral deviation control effort, causing the robot to approach the target with a larger curvature k. However, this increases heading deviation θ upon reaching the target, leading to oscillations and degraded tracking. Conversely, a large L_d results in a smaller curvature k and reduced heading deviation, which prevents oscillations near the target. However, it increases system response time (latency) and also degrades performance.

Consequently, a dynamically adjustable look-ahead distance L_d is crucial for varying deviation conditions. While methods like proportional control, Particle Swarm Optimization (PSO), and fuzzy control exist, PSO demands high computational resources and introduces latency, and fuzzy control requires complex

rule formulation and extensive experience. To simplify control, reduce computational load, and minimize latency, this study employs a proportional control method *(Yu et al., 2022)* for L_d selection, given by:

$$L_d = Gv + L_0 \quad (4)$$

where: G is the Adjustment ratio coefficient; and L_0 is the Preset lead distance [m].

The analysis shows that lateral deviation depends on L_d, operational speed v, turning radius, and wheelbase. As wheelbase is fixed, turning radius and L_d selection are linked to operational speed. Thus, stable operational speed directly impacts lateral deviation control and path tracking performance.

Weeding robots, typically electric motor-driven, face varying resistance from soil compaction during inter-row weeding. This causes sudden motor load changes, leading to fluctuations in motor speed and, consequently, robot operational speed. Therefore, a motor speed control algorithm with enhanced anti-interference capability is essential for stable operation in complex field environments.

Operational Speed Control System

Linear Active Disturbance Rejection Control (LADRC) *(Yuan et al., 2013)* is a bandwidth-based control strategy derived from the Nonlinear Active Disturbance Rejection Control (ADRC) technique. LADRC comprises a Tracking Differentiator (TD), a Linear Extended State Observer (LESO), and a Linear State Error Feedback (LSEF) control law. LADRC can theoretically adapt to multi-order or high-order systems. As the motor in this study is a second-order control plant, the structure of the second-order LADRC is presented below.

Let the uncertain second-order control plant model be represented as:

$$\mathrm{y} = f(x_1, x_2 x, w, t) + bu \quad (5)$$

where: u is the System Input; y is the System Output; w is the External disturbances to the system; b is the Control gain; and x_1,x_2 is the System Parameters.

The LADRC system comprises a Linear Extended State Observer (LESO) and a Linear State Error Feedback (LSEF) controller. The LESO estimates the internal and external disturbances in real-time, aggregating them into a total disturbance state.

Despite LADRC having fewer parameters (six) than ADRC, its tuning is more complex than traditional PID controllers. To address this, this paper proposes using an improved Northern Goshawk Optimization (NGO) algorithm to optimize LADRC's control parameters, aiming for superior performance.

Improved Northern Goshawk Optimization Algorithm

The Northern Goshawk Optimization (NGO) algorithm, proposed by *Mohammad Dehghani et al. (2021)*, is a swarm intelligence optimization algorithm. It simulates Northern Goshawk behaviors—prey identification (exploration), attack, pursuit, and escape (exploitation)—to find optimal solutions. NGO offers advantages like fast convergence, fewer control parameters, and robustness, adapting to specific problem characteristics with universality. Compared to traditional swarm intelligence algorithms, NGO better balances global and local exploration, quickly identifying optimal search regions for fine-grained searches.

Despite its strengths, NGO has limitations. Random, uneven initial solution distribution can reduce population diversity, and insufficient global search during prey identification often leads to local optima.

To address the aforementioned issues, this paper proposes the following improvements to the NGO algorithm:

First, initial population positions are randomly generated using a chaotic Tent map. This ensures a more uniform distribution, accelerates convergence, helps escape local optima, maintains diversity, and enhances global search.

Second, the Sine Cosine Algorithm (SCA) is integrated into NGO's prey identification phase. SCA leverages sine and cosine oscillatory characteristics to influence discoverer positions, maintaining diversity and improving global search capability by performing global and local optimization based on these oscillations to find the overall optimal value.

Standard NGO relies on stochastic exploration, which can lead to local optima. To enhance the global search capability, the Sine Cosine Algorithm (SCA) strategy is integrated into the exploration phase. The improved position update formula, which replaces the standard exploration mechanism, is expressed as:

$$X_{i,j}^{\mathrm{new},P_1} = \begin{cases} \omega \cdot X_{i,j} + r_1 \cdot \sin\ r_2 \cdot |r_3 \cdot X_{\mathrm{best}} - X_{i,j}|, R < ST \\ \omega \cdot X_{i,j} + r_1 \cdot \cos\ r_2 \cdot |r_3 \cdot X_{\mathrm{best}} - X_{i,j}|, R \geqslant ST \end{cases} \quad (6)$$

where:

ω is the proportional factor for position adjustment; r_1 is the step-size search factor that decreases linearly with iterations; r_2, r_3 are random numbers within the range [0,2π]; R is a random number within the range [0,1]; ST is the threshold determining the selection of the cosine strategy; and X_{best} is the Current Optimal Position.

This study uses the Integral of Time-weighted Absolute Error (ITAE) as the comprehensive evaluation metric, or fitness value. ITAE, a time-weighted integral of absolute error, is commonly used in optimized controller design to achieve smoother system responses. Minimizing ITAE allows for parameter adjustment to achieve superior system responses. The calculation formula is:

$$ITAE = \int_0^{\infty} t|e(t)|\,dt \tag{7}$$

where: t is the time; and $e(t)$ is the system error at time t.

RESULTS

Simulation Analysis

To verify the LADRC speed control algorithm's impact on path tracking, a comparative analysis was conducted between the traditional PID-based Pure Pursuit and LADRC-based Pure Pursuit algorithms, evaluating their characteristics and effectiveness.

Operational Speed Control Simulation

As the weeding robot's operational speed directly relates to motor rotational speed, operational speed control is essentially motor speed control. First, separate Simulink models for LADRC and PID motor speed control were established, as shown in Fig. 5. Then, NGO and INGO algorithms optimized their respective parameters to obtain optimal control settings. Using these parameters, operational speed control was performed for each controller, and their effects were compared. Both NGO and INGO used a population size of 30 and 100 maximum iterations. The Simulink sampling time was 0.01 s, with a step response input of 561, corresponding to 1 m/s operational speed.

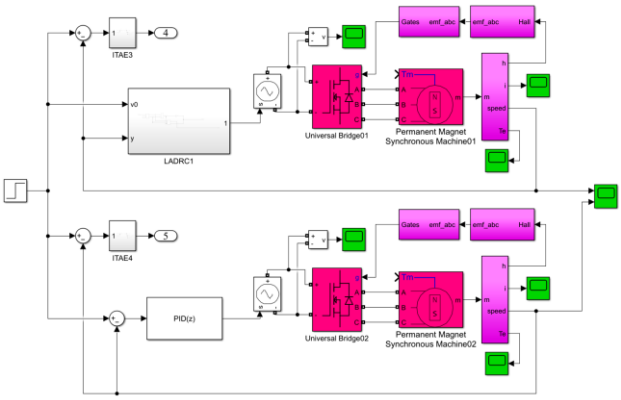

Fig. 5 - Simulink simulation model of LADRC and PID controller

Before optimization, LADRC and PID parameter ranges were manually tuned to reduce iterative optimization time. The Simulink simulation models for the LADRC and PID controllers are shown in Figure 5. The electrical parameters of the DC brushless motor are listed in Table 2.

Table 2

DC Brushless Motor Parameters

DC Brushless Motor Parameters	value
Types of Electric Motors	Three-phase brushless DC motor
Moment of inertia J / (kg·m^2)	5.3×10^{-3}
Torque coefficient K_T / (N·m/A)	1.66
Reverse Voltage Constant k_e / (V·m/r)	0.96
Armature Inductance L_A / (H)	0.1
Armature resistance $r_{A/}$ (Ω)	0.1
Damping coefficient B	2×10^{-4}

After these preparations, program execution results were analyzed. Fig. 6 shows the optimized fitness values for both controllers, obtained by NGO and INGO, while Figure 7 depicts the step response curves. LADRC's optimized fitness values were 0.0092 (NGO) and 0.0056 (INGO), while PID's were 1.0365 (NGO) and 1.0359 (INGO). Fig. 6 shows that INGO achieved smaller initial fitness values and converged faster than NGO, demonstrating its advantages in parameter optimization speed and local optima escape.

Due to INGO's superior optimization, INGO-optimized LADRC and PID parameters were directly used in the simulation for step response comparison. The step response curves show that LADRC reached steady-state earlier (0-0.05s) with 0.01% overshoot, compared to PID's 0.77%. This indicates LADRC's faster initial response, achieving the setpoint quicker with less overshoot.

To compare disturbance rejection, a 7-unit external disturbance was introduced at 0.2 s. Fig. 7 shows LADRC's motor speed overshot by 0.14% (0.2-0.2002 s) and largely recovered to steady-state by 0.2015 s. PID, however, saw overshoot increase to 5.91% (0.2-0.208 s), recovering only around 0.26 s. Thus, LADRC demonstrates faster recovery and stronger stability under disturbances in operational speed control.

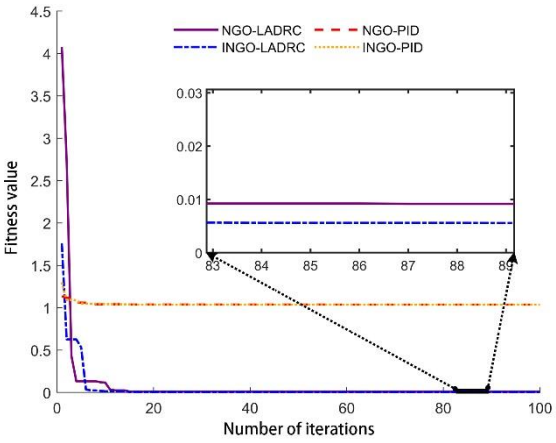

Fig. 6 - Fitness value change curve

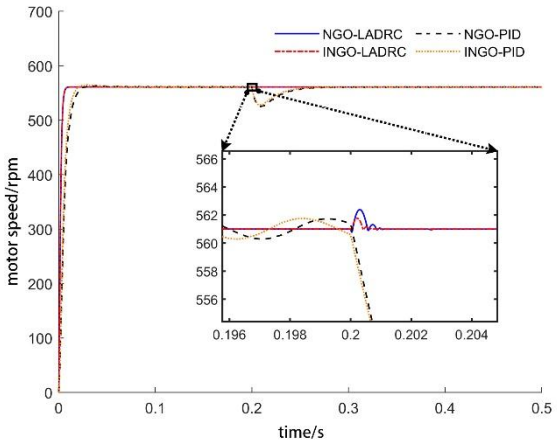

Fig. 7 - Step response curve

Path Tracking Simulation

The weeding robot's structural parameters (length, wheelbase) were input into MATLAB to establish the path tracking model. A 122.83 m S-shaped path, comprising three straight and two curved segments, was defined. Initial lateral and heading deviations were set to 1 m and 1.15°, respectively.

Operational speed control, set at 1 m/s using the optimized motor speed model, included disturbances: a continuous 10 N·m on straight segments and a sinusoidal torque (5 N·m amplitude, 5 N·m offset, 1 rad/s frequency) at turns to simulate turning effects. The path tracking curve and lateral error curve are shown in Fig. 8 and Fig. 9, respectively. The results of the lateral error analysis are presented in Table 3.

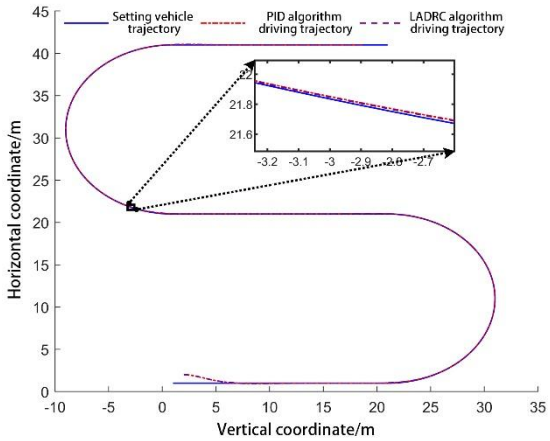

Fig. 8 - Path tracking driving trajectory

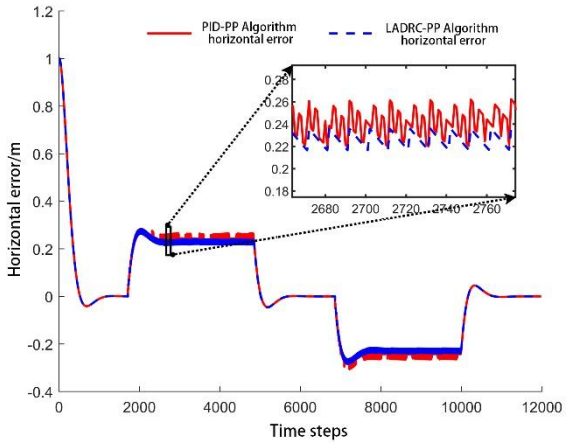

Fig. 9 - Lateral error in path tracking

Table 3

Lateral Error Statistics

Algorithm	Maximum error / m	Absolute Mean Error / m	Root Mean Square Error / m
PID-PP	0.2832	0.1512	0.2119
LADRC-PP	0.2820	0.1466	0.2066

Simulation results show that both LADRC-PP and PID-PP had an initial convergence time of 5.23 s. This consistency is attributed to fewer disturbances and similar speeds during this phase, resulting in comparable path tracking performance.

As shown in Figure 10 and Table 3, LADRC-PP significantly reduced lateral error compared to PID-PP. Specifically, LADRC-PP's RMSE, MAE, and maximum error were reduced by 2.5%, 3%, and 0.42%, respectively. The small reduction in maximum error suggests similar performance under high-curvature paths, where both algorithms' response capabilities saturated. Overall, LADRC-PP demonstrated superior performance in maximum, mean absolute, and root mean square lateral errors, despite similar initial convergence times. This leads to better path tracking performance.

Field Experiments

Field experiments validating LADRC-PP's path tracking performance were conducted on June 12, 2023, at Heilongjiang Bayi Agricultural University's experimental farm. The experimental field had a ridge width of 1.1 m and a ridge height of 0.2 m. The cultivated crop was soybean, planted using a large ridge double-row method. The growth stage was the second node stage, with an average plant spacing of 4 cm. During the experimental tests, the weeding robot prototype was driven to the vicinity of the desired path's starting point. The field experiment setup for automatic navigation is shown in Fig. 10.

Fig. 10 - Field automatic navigation

During the experiments, the weeding robot's initial position relative to the path was set with a lateral deviation of 0.3 m and a heading deviation of 15°. The weeding robot performed path tracking on soybean seedling rows using both PID-PP and LADRC-PP algorithms at operational speeds of 1 m/s, 0.8 m/s, and 0.6 m/s. Three experimental sets were conducted for each algorithm, and average values were recorded. Evaluation metrics included initial convergence time, maximum lateral tracking error after stable convergence, mean absolute tracking error, and root mean square error. Results are in Table 4.

Table 4

Test results

Control Algorithm	Operating speed / (m/s)	Maximum error / m	Absolute Mean Error / m	Root Mean Square Error / m
PID-PP	1	0.0526	0.0283	0.0305
	0.8	0.0474	0.0252	0.0277
	0.6	0.0362	0.0164	0.0178
	mean	0.0454	0.0233	0.0253
LADRC-PP	1	0.0418	0.0211	0.0232
	0.8	0.0384	0.0192	0.0213
	0.6	0.0327	0.0137	0.0144
	mean	0.0376	0.018	0.0196

Table 4 shows LADRC-PP reduced maximum lateral error by 20.5%, 19%, and 9.67% at 1, 0.8, and 0.6 m/s, respectively, compared to PID-PP. Mean absolute error decreased by 25.4%, 23.8%, and 16.5%, and RMSE by 23.9%, 23.1%, and 19.1%. LADRC-PP's performance advantage diminishes at lower speeds because the vehicle's slower dynamic response and smaller tracking errors at low speeds allow PID to perform more effectively. In such low-speed environments, LADRC-PP's disturbance rejection and dynamic compensation benefits are less pronounced, reducing the performance difference between the algorithms. Overall, LADRC-PP's evaluation metrics consistently surpassed PID-PP's, validating its effectiveness.

However, it is important to note that the field experiments were conducted on relatively flat terrain. In extreme agricultural environments characterized by steep slopes or severe tire slip, the simplified kinematic model might be compromised, potentially limiting tracking stability.

CONCLUSIONS

(1) A path tracking control method based on the LADRC-PP algorithm was designed. The LADRC controller was used for real-time control of the weeding robot's motor speed, and the INGO optimization algorithm was employed to optimize the LADRC controller parameters. Compared to traditional PID controllers, the LADRC controller, by real-time estimation and compensation of external disturbances, can respond more quickly and recover to a normal state when facing disturbances. The LADRC-PP algorithm reduced path tracking errors caused by unstable operational speed, thereby improving overall path tracking performance.

(2) Simulation analysis of the control algorithms (before and after improvement) was conducted using MATLAB. The simulation results indicated that under the same initial deviation conditions, the LADRC-PP algorithm reduced the root mean square error of lateral deviation by 2.5%, the mean absolute error by 3.0%, and the maximum error by 0.42% compared to the PID-PP algorithm.

(3) Field experiments demonstrated that compared to the PID-PP path tracking algorithm, the LADRC-PP path tracking algorithm reduced the maximum lateral error by 20.5%, 19%, and 9.67% at operational speeds of 1 m/s, 0.8 m/s, and 0.6 m/s, respectively. The mean absolute error was reduced by 25.4%, 23.8%, and 16.5%, respectively, and the root mean square error by 23.9%, 23.1%, and 19.1%, respectively. The LADRC-PP path tracking algorithm exhibited advantages over the PID-PP path tracking algorithm in terms of maximum lateral error and root mean square error, with this advantage gradually diminishing as the operational speed decreased. It can be concluded that under actual field operating conditions, the LADRC-PP path tracking algorithm possesses stronger disturbance rejection capability against changes in resistance during operation. However, the advantage of the proposed algorithm diminishes at lower operating speeds. Future work will focus on validating the system in more complex terrains and varying soil conditions to further assess its robustness.

ACKNOWLEDGEMENT

This work was supported by Heilongjiang Provincial Natural Science Foundation Joint Guided Project (LH2023E105).

REFERENCES

[1] AbdElmoniem, A., Osama, A., Abdelaziz, M., Maged, S.A. (2020). A Path-tracking Algorithm Using Predictive Stanley Lateral Controller [J]. *International Journal of Advanced Robotic Systems*, Vol.17, No.6, pp. 1729881420974852.

[2] Ahn, J., Shin, S., Kim, M., Park, J. (2021). Accurate Path Tracking by Adjusting Look-ahead Point in Pure Pursuit Method [J]. *International Journal of Automotive Technology*, Vol.22, No.1, pp. 119-129.

[3] Dehghani, M., Hubálovský, Š., Trojovský, P. (2021). Northern Goshawk Optimization: A New Swarm-Based Algorithm for Solving Optimization Problems [J]. *IEEE Access*, Vol.9, pp. 162059-162080.

[4] Deshmukh, D., Kumutham, A.R., Pratihar, D.K., Deb. A.K. (2025). Accurate Path Tracing of a Tracked Robot: A Modified PID Approach with Slip Compensation [J]. *Engineering Research Express*, Vol.7, No.1, pp. 015203.

[5] Farag, W. (2020). Complex Trajectory Tracking Using PID Control for Autonomous Driving [J]. *International Journal of Intelligent Transportation Systems Research*, Vol.18, No.2, pp. 356-366.

[6] Fu, X.B., Han, Z.D., Han, K.L., Feng, X.B., Huang, T. (2023). Path Tracking of Improved Pure Pursuit Model of Wheeled Harvester Based on PSO Algorithm (基于粒子群算法改进的轮式收获机纯追踪模型

路径跟踪研究) [J]. *Agricultural Engineering*, Vol.13, No.07, pp. 105-112. DOI: 10.19998/j.cnki.2095-1795.2023.07.015

[7] Jain, H., Babel, P. (2024). A Comprehensive Survey of PID and Pure Pursuit Control Algorithms for Autonomous Vehicle Navigation [J]. *arXiv preprint arXiv*:2409.09848.

[8] Li, G., Wang, Y., Guo, L.F., Tong, J.H., He, Y. (2018). Improved Pure Pursuit Algorithm for Rice Transplanter Path Tracking (插秧机导航路径跟踪改进纯追踪算法) [J]. *Transactions of the Chinese Society for Agricultural Machinery*, Vol.49, No.05, pp. 21-26. Beijing/China.

[9] Li, T.C., Hu, J.T., Gao, L., L, X.G, Bai, X.P. (2013). Agricultural Machine Path Tracking Method Based on Fuzzy Adaptive Pure Pursuit Model (基于模糊自适应纯追踪模型的农业机械路径跟踪方法) [J]. *Transactions of the Chinese Society for Agricultural Machinery*, Vol.44, No.01, pp. 205-210. Beijing/China.

[10] Liu, J.J., Wang, Y., Li, G.Q., Zhang, Y.E., Yu, W., Fu, L.S. (2025). Analysis and Outlook of China's Soybean Supply and Demand Situation (中国大豆供需形势分析与展望) [J]. *Agricultural Economy*, No.10, pp. 124-126.

[11] Liu, Z.P., Zhang, Z.G., Luo, X.W., Wang, H., Huang, P.K., Zhang, J. (2018). Design of automatic navigation operation system for Lovol ZP9500 high clearance boom sprayer based on GNSS (雷沃 ZP9500 高地隙喷雾机的 GNSS 自动导航作业系统设计) [J]. *Transactions of the Chinese Society for Agricultural Machinery*, Vol.34, No.01, pp. 15-21. Beijing/China.

[12] Macenski, S., Singh, S., Martín, F., Ginés, J. (2023). Regulated Pure Pursuit for Robot Path Tracking [J]. *Autonomous Robots*, Vol.47, No.6, pp. 685-694.

[13] Ni, J., Wang, Y., Li, H., Du, H.L. (2022). Path Tracking Motion Control Method of Tracked Robot Based on Improved LQR Control [C]//*2022 41st Chinese Control Conference (CCC). IEEE*, pp. 2888-2893.

[14] Pan, S.J., Li, Y.L., Li, Z.X., Li, J.S, Xu, Y.C. (2022). Path Following Method of Intelligent Vehicles Based on Fuzzy Regulation (基于模糊调节的智能车路径跟随方法) [J]. *Journal of Military Transportation*, Vol. 1, No.10, pp. 78-83.

[15] Peicheng, S., Li, L., Ni, X., Yang, A.X. (2022). Intelligent Vehicle Path Tracking Control Based on Improved MPC and Hybrid PID [J]. *IEEE Access*, Vol.10, pp. 94133-94144.

[16] Rokonuzzaman, M., Mohajer, N., Nahavandi, S. (2023). Effective Adoption of Vehicle Models for Autonomous Vehicle Path Tracking: A Switched MPC Approach [J]. *Vehicle System Dynamics*, Vol.61, No. 5, pp. 1236-1259.

[17] Shen, Y., Zhao, S., Zhang, Y.F., He, S.W., Feng, R., Liu, H. (2024). Improved Pure Tracking Control of Four-wheel Synchronous Steering Agricultural Machinery Based on Variable Forward Looking Distance (基于变前视距离的四轮同步转向农机改进纯跟踪控制) [J]. *Transactions of the Chinese Society for Agricultural Machinery*, Vol.55, No.03, pp. 21-28. Beijing/China.

[18] Wang, H., Wang, G.M., Luo, X.W., Zhang, Z.G., Gao, Y., He, J., Yue, B.B. (2019). Path tracking control method of agricultural machine navigation based on aiming pursuit model (基于预瞄追踪模型的农机导航路径跟踪控制方法) [J]. *Transactions of the Chinese Society for Agricultural Machinery*, Vol.35, No.04, pp. 11-19. Beijing/China.

[19] Wang, L., Zhai, Z., Zhu, Z., Mao, E.R. (2022). Path Tracking Control of an Autonomous Tractor Using Improved Stanley Controller Optimized with Multiple-population Genetic Algorithm [C]//*Actuators. MDPI*, Vol.11, No.1, pp. 22.

[20] Xiao, S.D., Jiang, H.F., Du, J.L., Wang, H.Y., Meng, X.Y., Xiong, Y. (2023). Path Tracking Algorithm of Agricultural Vehicle Based on Two Stages Pure Tracking Model (基于两阶段纯追踪模型的农用车辆路径跟踪算法研究) [J]. *Transactions of the Chinese Society for Agricultural Machinery*, Vol.54, No.04, pp. 439-446+458. Beijing/China.

[21] Yang, Y., Li, Y., Wen, X., Zhang, G., Ma, Q.L., Cheng, S.K., Qi, J., Xu, L.Y., Chen, L.Q. (2022). An Optimal Goal Point Determination Algorithm for Automatic Navigation of Agricultural Machinery: Improving the Tracking Accuracy of the Pure Pursuit Algorithm [J]. *Computers and Electronics in Agriculture*, Vol. 194, pp. 106760.

[22] Yu, L.Y., Wang, X.Y., Wu, B.G., Hou, Y.Z., Wu, Y.H. (2022). Path planning optimization and tracking of parallel parking for driverless vehicle (无人驾驶汽车平行泊车路径规划优化与跟踪) [J]. *Journal of Jiangsu University (Natural Science Edition)*, Vol.43, No.05, pp. 519-523.

[23] Yuan, D., Ma, X.J., Zeng, Q.H., Qiu, X.B. (2013). Research on frequency-band characteristics and parameters configuration of linear active disturbance rejection control for second-order systems (二阶系统线性自抗扰控制器频带特性与参数配置研究) [J]. *Control Theory & Applications*, Vol.30, No.12, pp.1630-1640.

[24] Zhang, C.Y., Dong, W.J., Xiong, Z.Q., Hu, Z.Q., Wang, D.H., Ding, Y.C. (2021). Design and Experiment of Fuzzy Adaptive Pure Pursuit Control of Crawler-type Rape Seeder (履带式油菜播种机模糊自适应纯追踪控制器设计与试验) [J]. *Transactions of the Chinese Society for Agricultural Machinery*, Vol.52, No.12, pp. 105-114. Beijing/China.

[25] Zhang, H.Q., Wang, G.D., Lv, Y.F., Qin, C.L., Liu, L., Gong, J.L. (2020). Agricultural Machinery Automatic Navigation Control System Based on Improved Pure Tracking Model (基于改进纯追踪模型的农机路径跟踪算法研究) [J]. *Transactions of the Chinese Society for Agricultural Machinery*, Vol.51, No.09, pp. 18-25. Beijing/China.

[26] Zhang, W.Y., Ding, Y.C., Wang, X.L., Zhang, X., Cai, X., Liao, Q.X. (2016). Pure Pursuit Control Method Based on SVR Inverse-model for Tractor Navigation (基于 SVR 逆向模型的拖拉机导航纯追踪控制方法) [J]. *Transactions of the Chinese Society for Agricultural Machinery*, Vol.47, No.01, pp. 29-36. Beijing / China.